

Environmental Forensics

ISSN: 1527-5922 (Print) 1527-5930 (Online) Journal homepage: https://www.tandfonline.com/loi/uenf20

Determination of water quality assessment in wells of the Göksu Plains using multivariate statistical techniques

Esra Deniz Güner, Hatice Oncel Cekim & Galip Seçkin

To cite this article: Esra Deniz Güner, Hatice Oncel Cekim & Galip Seçkin (2021) Determination of water quality assessment in wells of the Göksu Plains using multivariate statistical techniques, Environmental Forensics, 22:1-2, 172-188, DOI: 10.1080/15275922.2020.1834025

To link to this article: https://doi.org/10.1080/15275922.2020.1834025

Published online: 17 Nov 2020.

Submit your article to this journal

Article views: 154

View related articles

View Crossmark data

Citing articles: 2 View citing articles

Full Terms & Conditions of access and use can be found at
https://www.tandfonline.com/action/journalInformation?journalCode=uenf20

ENVIRONMENTAL FORENSICS
2021, VOL. 22, NOS. 1–2, 172–188
https://doi.org/10.1080/15275922.2020.1834025

Taylor & Francis
Taylor & Francis Group

Check for updates

Determination of water quality assessment in wells of the Göksu Plains using multivariate statistical techniques

Esra Deniz Güner[a], Hatice Oncel Cekim[b], and Galip Seçkin[a]

[a]Environmental Engineering Department, Cukurova University, Adana, Turkey; [b]Department of Statistics, Hacettepe University, Ankara, Turkey

ABSTRACT

Groundwater is one of the most important sources of freshwater globally and has a key role in sustaining the ecological value of many areas. These valuable and vulnerable groundwater resources are under the pressure of many external pollution threats, such as industrial, domestic, and agricultural chemicals. To prevent undesirable consequences to future groundwater resources, comprehensive and proper knowledge of groundwater quality and contamination levels is vital at the local/regional scale. In this study, multivariate statistical techniques, such as a correlation matrix, hierarchical cluster analysis, and factor analysis, were applied to water quality data sets obtained from 24 wells located in the Göksu Plain. These techniques were applied primarily to nineteen hydrochemical parameters collected between May 2011 and April 2012. The results obtained from the correlation matrix showed that the seawater descriptors such as EC, TDS, Cl^-, Na^+, and K^+ were strongly correlated. Principal component analysis indicated that most of the variations in groundwater were caused by four factors that were responsible for the water quality, which represented more than 80.22% of the total data variance. The hierarchical average linkage cluster analysis produced two major clusters that reflected seawater salinity.

KEYWORDS

Seawater intrusion; coastal aquifer; multivariate analysis; hierarchical cluster analysis; factor analysis

Introduction

Groundwater resources are precious and particularly vulnerable resources used in many areas such as irrigation of crops and pastures, industrial and drinking water consumption, and ecological services (Siebert et al., 2010; De Stefano et al., 2015). Groundwater resources are important alternative water sources in coastal areas. Coastal areas generally attract the majority of the population due to favorable living conditions and economic activities (agricultural, trade, and tourism). This usually causes an increase in water demand for consumption in coastal areas. Therefore, groundwater resources in coastal areas are under growing pressure from excessive groundwater extraction (Shi and Jiao, 2014; Morgan and Werner, 2015; Qi et al., 2019). Thus, over-pumping of coastal aquifers may damage the seawater–freshwater interface equilibrium, which in turn may cause seawater intrusion (Huang et al., 2015; Liu et al., 2018; Tully et al., 2019; Hounsinou, 2020). Seawater intrusion in coastal alluvial aquifers causes groundwater quality deterioration, salinization, low productivity, and reduction of fresh water (Kang and Jackson, 2016; Ros and Zuurbier, 2017; Sae-Ju et al., 2020). In particular, because of excess groundwater extraction and increasing salinization, non-renewable groundwater in the coastal aquifer zone is endangered. The consequence is that people face a serious drinking water crisis due to freshwater salinization in coastal aquifers (Talukder et al., 2016; Rakib et al., 2020).

Various methodologies such as numerical modeling, geophysical and hydrochemical techniques, observations, lab experiments, and theoretical studies have been conducted to assess seawater intrusion in coastal aquifers (Jeong et al., 2010; Gong and Shen, 2011; Werner et al., 2011; Zhang et al., 2011; Cheng et al., 2012; Cai et al., 2015; Eissa et al., 2016; Kazakis et al., 2016; Fadili et al., 2017; Najib et al., 2017). In addition, many different statistical analyses, such as multivariate statistical analysis, cluster analysis, principal component analysis (PCA), and factor analysis (FA) have been used successfully to determine the changes in quality and pollution in surface water and groundwater (Bhuiyan et al., 2011; Arslan, 2013; Belkhiri and Narany, 2015; Telahigue et al., 2018; Sae-Ju et al.,

CONTACT Esra Deniz Güner eguner@cu.edu.tr
© 2020 Informa UK Limited, trading as Taylor & Francis Group

2020). Additionally, statistical techniques can be successfully applied to identify anthropogenic and geogenic phenomena influencing groundwater hydrochemistry (Moyo, 2013; Seanego and Moyo, 2013; Palma et al., 2014; Dragon and Gorski, 2015; Souid et al., 2018).

Rakib et al. (2020) used instrumental and statistical tools to determine the basic pollution parameters in 26 groundwater samples from Shyamnagar Sub-District (Bangladesh). The results showed that the pollution could be divided into two main groups of factors. One group contained salinization factors such as EC, TDS, Cl^-, SO_4^{2-}, NO_2^-, Br^-, F^-, Pb, Fe, As, Ca^{2+}, and temperature, while the other group included Zn, Mn, PO_4^{3-}, and Li related to groundwater quality. Busico et al. (2020) used multivariate statistical and regression analyses to delineate the specific vulnerability to anthropogenic pollution (SVAP) and weighting anthropogenic factors in the Florina Basin (Greece) and the Garigliano River Basin (Italy). Using these techniques, they successfully separated groundwater resources into those related to seawater intrusion, interaction with igneous sediments, and anthropogenic impact by grouping the water samples according to their characteristics. Selle et al. (2013) examined spatial and temporal patterns of principal component (PC) scores to improve the understanding of processes governing groundwater quality in the Ammer catchment located in southwest Germany. The results delineated the influence of land use and geology on groundwater quality. Kim et al. (2014) used model-based cluster analysis to understand the contributions of natural and anthropogenic factors to groundwater quality in South Korea. The results showed that the bivariate normal mixture model was more valid than multivariate analysis, and provided better identification between anthropogenic and natural groundwater groups. Souid et al. (2018) stated that there is a strong relationship between seawater intrusion in coastal aquifers and lithium by geochemical modeling and multivariate statistical analysis. According to the study results, seawater intrusion, evaporation, carbonate dissolution, and cation exchange interactions between groundwater and intercalated clay layers are the dominant factors in the aquifer materials. Sae-Ju et al. (2020) applied HFE-Diagram and PCA to successfully explain intrusion and freshening mechanisms in coastal aquifers in the Cha-Am District in Phetchaburi Province (Thailand). According to the level of impact of seawater intrusion, the geochemical evolution of groundwater is governed by three factors: (1) Ca^{2+}-Na^+-HCO_3^- and (2) Ca^{2+}-HCO_3^--Cl^- (slightly impacted), and (3) Na^+-Cl^- (highly impacted). Machiwal and Jha (2015) identified spatio-temporal variations in fifteen groundwater quality parameters in Udaipur district (India) by using PCA scores, box-and-whisker plots, and GIS-based geostatistical modeling. Box-and-whisker plots indicate that the hardness in groundwater exceeds its permissible limit at most sites in the aquifer system. The results of HCA successfully classified 53 sites into two clusters, in which cluster II is affected by natural geologic processes, and the groundwater of cluster I is contaminated by anthropogenic sources. Telahigue et al. (2018) explained salination and saltwater intrusion using hydrogeochemical and multivariate statistical analysis in the coastal aquifer. These authors identified two groups of water types as Ca-Mg-Cl-SO_4 in the middle of the island and Na-K-Cl on the nearby coast. Statistical analysis verified that the high groundwater mineralization was the result of seawater intrusion and gypsum and carbonate dissolution. Magyar et al. (2013) applied multivariate statistical methods to determine water quality in Neusiedler See, in Austria. They stated that most of the variance in the dataset could be explained by the main components (ions) and eight different areas that were distinguished. Using Wilk's lambda statistics, it was verified that the ions were mainly responsible for the formation of the previously discussed cluster groups.

Previous studies in this area have focused mainly on evaluating the groundwater chemical status in a water framework directive (Demirel, 2007; Seckin et al., 2010; Yilmaz et al., 2010). These authors concluded that the deterioration in water quality in some areas close to the sea was due to seawater intrusion and the intense use of groundwater for irrigation. However, these data have not been assessed using statistical methods, and water quality parameters have not been classified according to importance levels.

As a specially protected environmental area, the Göksu Plain is an important natural reserve and one of the most important natural wetlands in the Mediterranean region considering Turkey's historical, cultural, and social values. The Göksu Plain was included in the 1994 statute of the Convention on Wetlands of International Importance (Ramsar) as a water habitat in order to aim to ensure the sustainable use of these areas. Considering the bird species hosted in the past, this area is classified as a class "A" wetland (according to the Ramsar Convention, waterfowl wetlands hosting more than 25,000 species are class "A" wetlands). Similar to the Göksu Plain, Silifke is located on the Turkish Mediterranean coast and

supports the production of more than twenty types of agricultural crops due to its high fertility characteristics. With its productive alluvial soils and favorable climatic conditions, the Göksu Plain can produce a wide range of products twice or thrice yearly. The general trends that provide insight into the structure of the variables must be measured continuously and monitored systemically (Sargaonkar and Deshpande, 2003; Simeonov et al., 2003; Giardino et al., 2007).

In this study, the data set in the study by Güner et al. (2018) was used. In this data set, the water quality was analyzed using samples collected from 24 wells in Göksu Plain. Over the period of a year (May 2011 - April 2012) a total of nineteen physical and chemical water quality parameters were analyzed. However, when the seasonal and agricultural impacts of the region are taken into consideration, the average annual monthly data collected in this study were used to reflect the veracity of the results.

Determining the status of water resources and developing solutions to problems that arise will be easier using multivariate statistics. The intended purposes of the study were as follows: (1) to collect monthly water samples from the wells and classify the wells by water quality according to their change throughout one year and also classify hydrochemical parameters for changes in the wells using cluster analysis. (2) To determine the basic parameters affecting the water quality in the wells using FA and to identify these parameters in the saline fields in the study area where they are more dominant using cluster analysis. (3) To identify field properties with the aid of diagrams through an evaluation of basic parameter fractions to determine whether there is any seawater intrusion.

Materials and methods

Study area

The Göksu Plain is an important ecological and aesthetic resource along the Mediterranean coast. This plain provides fish and wildlife nurseries and habitat, forms storm buffers, filters many waterborne contaminants, and is important to coastal food chains. The Göksu Plain, which has a drainage area of 10,000 km^2, is located south of Silifke (Southern Anatolia). The locations of samples shown in Figure 1 and the geographical positions of the wells are also given in Table 1.

The geological formations in this area, which have different lithological properties, are aged from the first to the third phase of its geological history, and most of the area is covered by sedimentary rocks (medium hard-soft) that were deposited during the Miocene. The Göksu Plain was formed by the deposition of alluvial material carried by the Göksu River. Alluvial soils show that the rocks were primarily transported. River plains such as the Göksu Plain usually consist of high levels of calcareous structures. Therefore, the majority of alluvial soil is limestone.

The Mediterranean climate is dominant in this region. Summer is hot and arid, and winter is rainy and mild. The total annual precipitation is 606.8 mm, the average temperature is 21 °C, and the average evaporation is 1745 mm. The average climatic data for the study area are presented in Table 2.

Physical and chemical analyses

Samples were collected monthly between May 2011 and April 2012 from 24 wells located in the Göksu Plain. At each sampling station, the temperature (T; °C), pH, and electrical conductivity (EC; μS cm^{-1}) of the water samples were measured in the field using WTW pH340 and 2510-A Orion instruments. The amount of total dissolved solids (TDS) was determined by filtering the samples through Whatman (0.45 μm) filter paper, followed by evaporation for 24 h at 150 °C in pre-conditioned and pre-weighed crucibles.

The change in weight was used to determine the dissolved salts. The alkalinity was analyzed by titration (CO_3^{2-}, HCO_3^-) using the alkalinity (2320)/titration S.2-35 standard method. For ion analysis, nitric acid was added to each water sample to ensure a pH <2. The bottles were tightly capped to prevent the intrusion of atmospheric CO_2. All samples were transported to the Environmental Chemistry Laboratory of Cukurova University and stored in a refrigerator at 4 °C until analysis. All major cations, including Ca^{2+}, Mg^{2+}, Na^+, K^+, Si, and Ba were analyzed using a Perkin Elmer highly sensitive inductively coupled plasma spectrometer (ICP), and anion concentrations for SO_4^{2-}, NO_3^-, and Cl^-, were measured using ion chromatography (IC), following the Water Environment Federation and American Public Health Association (2005). While performing the analysis, each sample was analyzed in triplicate and two sets of internal standards were run at the beginning and during the analysis, to check the accuracy and precision of the results. For most of the elements, the detection limits were approximately 1 ppb and the estimated analytical errors were within 5%.

The sodium adsorption ratio (SAR) was used in the classification of water, and the residual sodium carbonate (RSC) and %Na were calculated according to the formulas below. All ionic values used in these formulas are in meq/L.

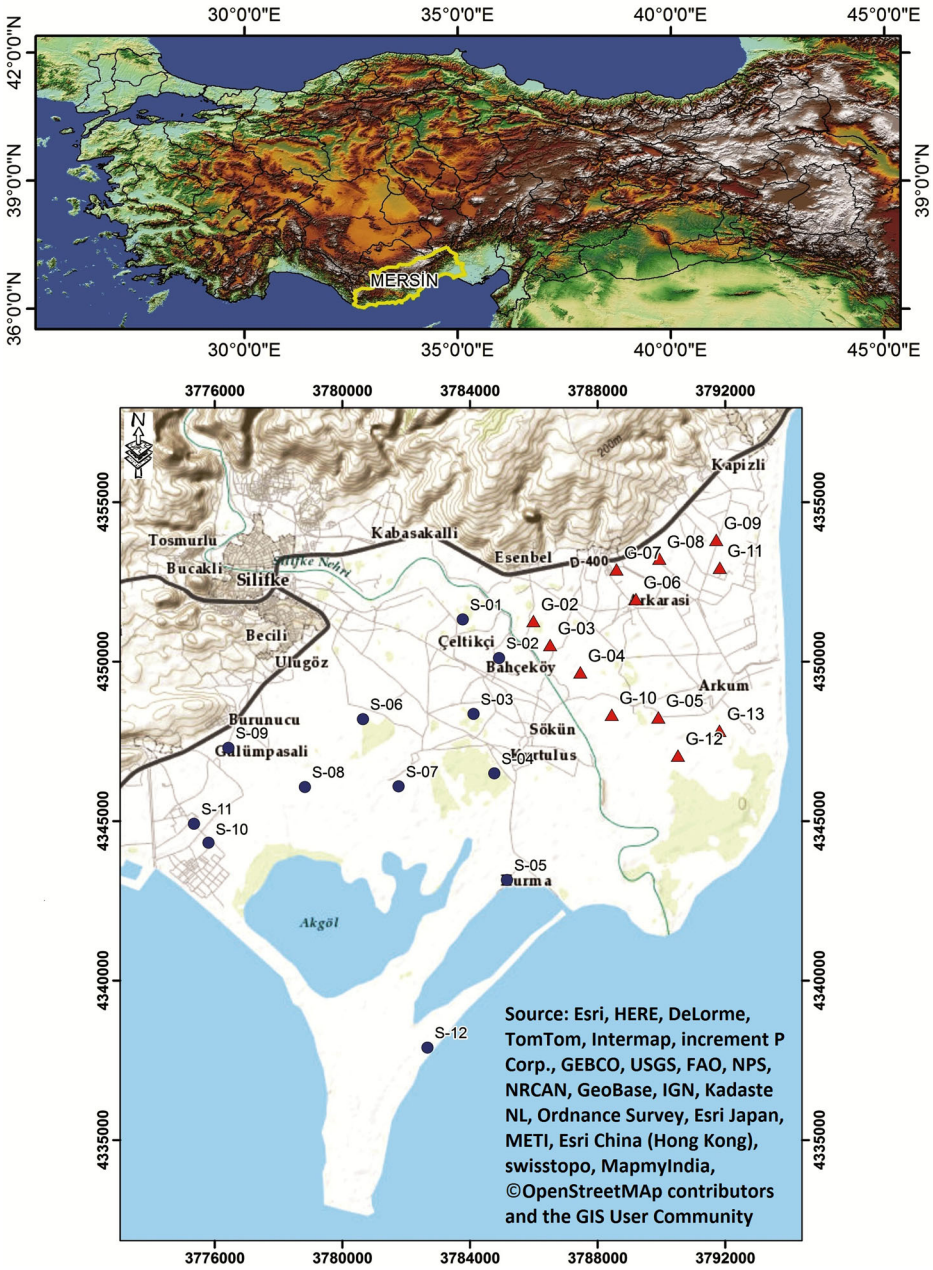


Figure 1. The locations of samples in the Göksu Plains.

The SAR was calculated using the following formula (Raghunath, 1987):

$$SAR = \frac{Na^+}{\sqrt{\frac{Ca^{2+}+Mg^{2+}}{2}}} \quad (1)$$

The RSC was determined as follows (Eaton, 1950):

$$RSC = (CO_3^{2-} + HCO_3^-) - (Ca^{2+}+Mg^{2+}) \quad (2)$$

The %Na was determined as follows (Wilcox, 1955):

$$\%Na = \frac{100 \times Na^+}{Na^+ + Ca^{2+} + K^+ + Mg^{2+}} \quad (3)$$

Statistical analysis

The data were transformed to ensure suitability for proper statistical tests. In many statistical tests, the assumption of normal distribution should be provided; therefore, the data were logarithmically transformed to eliminate the measurement unit differences between the data. The Shapiro-Wilk test indicated that the P-value (=99%) exceeded 0.01, indicating that the data were normally distributed. Similarly, Kaiser–Meyer–Olkin (KMO) and Bartlett's tests were used to determine whether the data were suitable for FA analysis. The KMO value was 0.50, and Bartlett's

Table 1. Geographical positions of the wells in the Göksu Plain.

Location-well	Elevation (m)	Latitude (North)			Longitude (East)		
G-01	6.0	36°	21′	41.01″	34°	1′	4.04″
G-02	7.0	36°	21′	10.04″	34°	1′	8.15″
G-03	43.0	36°	20′	59.56″	34°	1′	18.99″
G-04	44.0	36°	21′	1.55″	34°	1′	54.37″
G-05	42.0	36°	20′	32.61″	34°	2′	30.95″
G-06	8.0	36°	21′	48.83″	34°	2′	44.69″
G-07	32.0	36°	22′	13.45″	34°	2′	24.56″
G-08	17.5	36°	22′	15.98″	34°	2′	45.88″
G-09	40.0	36°	22′	22.35″	34°	2′	56.72″
G-10	41.0	36°	20′	44.84″	34°	1′	59.84″
G-11	43.0	36°	22′	18.55″	34°	2′	58.6″
G-12	65.0	36°	20′	11.47″	34°	3′	36.5″
G-13	60.0	36°	20′	11.16″	34°	3′	37.07″
S-01	55.0	36°	21′	50.77″	33°	59′	17.01″
S-02	30.0	36°	21′	50.66″	33°	59′	48.69″
S-03	75.0	36°	20′	17.81″	33°	59′	56.73″
S-04	35.0	36°	19′	49.19″	34°	0′	16.49″
S-05	49.0	36°	18′	25.09″	34°	0′	3.74″
S-06	30.0	36°	20′	53.71″	33°	57′	29.18″
S-07	38.0	36°	20′	31.59″	33°	57′	39.08″
S-08	30.0	36°	19′	59.36″	33°	56′	39.26″
S-09	42.0	36°	20′	9.02″	33°	55′	18.82″
S-10	4.0	36°	19′	1.88″	33°	55′	10.45″
S-11	12.5	36°	19′	13.33″	33°	54′	55.87″

Table 2. The annual average values of meteorological parameters in the Göksu Plain between May 2011 and April 2012. Güner et al. (2018).

	Temperature (°C)	Relative humidity (%)	Precipitation (mm)
Maximum	25.4	77.1	6.8
Minimum	17.0	30.1	0.3
Average	21.0	55.5	1.8

test of sphericity resulted in a chi-square value of 723.401 (P value = 0.000).

Combining many variables associated with each other, FA is a statistical method that allows for the identification of few, new, unrelated, or conceptually significant variables (factors, dimensions). Here, the most important factor is determining the number of PCs. The calculation of the stated variance and deciding on the number of components (factors) with eigenvalues of 1 or larger than 1 are both considered important factors. FA is a multivariate statistical technique to obtain a smaller number of meaningful variables from a larger number of variables and is intended to measure the same structure or property. The factors obtained in this analysis are assessed as strong if $f > 0.75$, medium if $0.50 < f < 0.75$, and weak if $0.30 < f < 0.50$. The important factors obtained in this study were subjected to Varimax rotation to provide independence, significance, and clarity in the interpretation.

The Pearson coefficient (r) was used to evaluate the statistical significance of the measured correlation values and to provide information on the strength and direction of linear relationships. Hierarchical cluster analysis (HCA) was used in this study, the Euclidean distance and Ward's clustering algorithm were selected, and the drainage channels of the data were converted into standardized Z scores. All of the mathematical and statistical computations were performed using IBM SPSS Statistics 23 version (License server: spss.hacettepe.edu.tr).

Results and discussion

A descriptive statistical overview of the hydrochemical data of the groundwater, which was sampled from May 2011 to April 2012 and includes major cations and anions, is presented in Table 3. The annual distributions of the water quality were evaluated with the minimum, maximum, mean, and standard deviation values for the considered variables. The water samples obtained from the wells in the study area had pH values ranging from 7.5 to 8.19 with mean ± SD of 7.82 ± 0.2, which indicates slight alkalinity. It is understood that the pH of seawater is >7, which is weakly alkaline. The relatively low alkalinity associated with groundwater in the Göksu Plain zone is caused by seawater intrusion. The well water samples were moderately hard with high EC, and TDS varied over a wide range of 265.5 to 5677.5 μS cm^{-1} and 156.6 to 3941.3 mg/L with an overall mean ± SD of 807.8 ± 839.6 mg/L and 1471.7 ± 1289.9 μS cm^{-1}, respectively. The average annual values Ca^{2+} and Mg^{2+} ranged from 15.83 to 136.43 mg/L and 13.4 to 125.6 mg/L, with mean ± SD of 62.44 ± 36.05 and 39.53 ± 26.79 mg/L, respectively. The Ca^{2+} content was

Table 3. Analytical results of the water quality parameters from the Göksu Plain.

Sample point	T	PH	EC	TDS	Ca^{2+}	Mg^{2+}	K^{+}	Na^{+}	Cr	SO_4^{2-}	NO_3^{-}	HCO_3^{-}	CO_3^{2-}	Ba	Si	B
G-01	20.69	7.68	1014	605.15	88.61	51.91	5.05	31.6	94.8	228.78	12.39	347.9	5.93	0.72	2.39	0.78
G-02	20.18	7.66	1324.58	796.88	100.43	48.04	5.69	77.5	127.74	251.29	12.2	381.62	2.58	0.5	2.56	0.89
G-03	20.28	8	667.42	574.69	85.52	45.52	4.89	88.2	212.77	169.26	12.13	191.13	17.6	0.19	2.12	0.65
G-04	20.38	7.96	883.67	392.82	78.23	20.56	4.88	108.7	94.02	226.57	12.14	211.25	17.12	0.26	2.37	0.64
G-05	21.2	7.6	1632	817.65	15.83	14.77	7.43	282.03	308.89	171.98	12.36	311.03	5.58	0.23	3.87	0.88
G-06	22.75	7.63	1208.5	728.74	63.66	48.29	14.66	89.34	98.5	253.67	12.21	453.72	2.05	0.46	2.92	0.88
G-07	21.23	8.02	1106.17	555.87	43.61	63.39	11.69	191.67	171.61	321.53	12.12	285.65	11.43	0.23	2.85	0.83
G-08	20.81	8.19	1014	523.32	21.39	20.46	13.59	134.25	136.69	138.67	12.42	240.43	22.42	0.22	3.15	0.88
G-09	20.35	8.02	1171.43	548.93	19.36	21.55	13.85	149.1	154.93	150.99	12.06	251.86	11.78	0.06	3.38	0.8
G-10	20.39	7.99	832.08	405.14	21.55	19.28	6.19	110.4	111.92	124.11	12.1	229.03	14.43	0.25	2.63	0.68
G-11	20.92	8.12	1104.92	551.18	28.07	18.22	11.3	155.93	123.13	245.67	12.51	264.87	21.38	0.2	3.33	0.87
G-12	22.3	7.68	5677.5	3941.3	124.8	125.64	34.46	880.11	1597.57	299.78	12.41	211.58	2.33	0.49	2.26	1.31
G-13	22.33	7.75	4629.17	2695.07	100.82	96.22	31.76	741.76	1279.42	207.76	12.94	233.98	4.98	0.47	2.14	1.72
S-01	20.74	7.75	753.33	322.7	56.28	31.54	3.27	25.72	112.64	105.61	12.56	233.55	9.55	0.4	3.47	0.64
S-02	20.71	7.71	949.75	488.31	136.43	64.44	4.2	42.05	185.13	249.97	12.73	289.22	5.08	0.94	2.24	0.69
S-03	20.53	7.83	1429.33	610.05	44.36	44.39	3.02	169.25	332.06	123.28	13.02	205.2	7.63	0.69	2.61	0.64
S-04	22.68	7.94	1277.58	568.92	37.35	27.65	5.99	149.6	254.34	130.78	13.31	196.45	13.8	0.38	2.58	0.72
S-05	22.04	8.18	3352.5	1517.11	36.68	29.98	20.44	451.96	543.51	223.46	13.34	267.6	23.1	0.37	3.89	1.44
S-06	21.6	7.84	265.57	156.61	31.57	13.4	4.66	411.14	100.51	302.31	12.33	77.75	9.88	0.14	0.8	0.41
S-07	20.91	7.91	601.25	256.4	45.06	25.96	2.41	31.8	72.02	114.17	12.47	203.53	9.97	0.21	2.36	0.55
S-08	20.68	7.57	633.42	308.15	36.86	16.64	2.71	53.44	77.32	115.7	12.54	221.73	2.6	0.7	1.67	0.64
S-09	23.13	7.56	924.75	528.17	96.81	30.69	6.32	19.51	123.47	160.68	12.68	260.67	2.57	0.43	2.03	0.55
S-10	21.34	7.67	2041.58	994.67	74.45	34.29	5.11	255.51	362.65	205.84	12.5	273.57	2.58	0.29	1.99	0.78
S-11	22.37	7.5	827.33	501.29	110.75	35.84	2.51	23.54	145.61	181.38	12.32	305.5	2.48	0.29	1.66	0.58

The water temperature (T) is in °C, electrical conductivity (EC) is in μS cm^{-1} and the other parameters are in mg/L.

higher in the limestone bedrocks and the Mg^{2+} content was higher in the dolomite area (Jiang et al., 2009; Sae-Ju et al., 2020). As shown in Table 3, there was more limestone than dolomite in the study area because Ca^{2+} and Mg^{2+} exhibited the same trends in concentration. The Na^{+} and K^{+} values ranged from 19.51 to 880.1 mg/L and 2.41 to 34.46 mg/L, with mean ± SD of 194.75 ± 222.5 and 9.42 ± 8.65 mg/L, respectively. Na^{+} was relatively abundant compared to Ca^{2+}. This may indicate very high TDS, hardness, and alkalinity of the water samples.

From a careful observation of these data, it is clear that the Na^{+}, Mg^{2+}, Cl^{-}, and SO_4^{2-} ions showed a wide range of distributions and higher standard deviations (SO_4^{2-} and Cl^{-} have mean ± SD of 195 ± 64.83 mg/L and 284.2 ± 375.4 mg/L, respectively). This suggests a possible incursion of nearby saline water, which has comparatively higher concentrations of Na^{+}, Mg^{2+}, Cl^{-}, and SO_4^{2-} (Table 3). Higher EC and TDS values were recorded in wells located near the sea. However, another reason for the high concentrations of Mg^{2+} is that limestone, which is dominant in this region, contains high amounts of Mg^{2+}.

Water quality was classified into four classes according to the Turkish Water Pollution Control Regulation (Anonymous, 1988). The water quality of class 1 is considered to be clean; the water quality of class 2 corresponds to a low pollution status; the water quality of class 3 corresponds to a polluted status, and the water quality of class 4 is considered to be highly polluted. According to the water quality based on the class guidelines and the annual average concentrations (Table 4), Na^{+}, Cl^{-}, and NO_3^{-} in the study area were classified as class 3 (polluted status) (Table 4). The TDS and SO_4^{2-} values included low pollution (class 2), while the other parameters showed clean water quality (class 1). The presence of Na^{+}, Cl^{-}, NO_3^{-}, and SO_4^{2-} can be explained as the result of agricultural, domestic wastewater, and possibly seawater intrusion.

Box-and-whisker plots (Figure 2) were used to display statistical summaries of the major elements in the groundwater samples. The central box represents the values from the lower to upper quartile (25th to 75th percentile). The middle line represents the median. The vertical line extends from the minimum to the maximum values.

The relationships between the measured hydrochemical parameters were obtained using correlation analysis (Table 5). Pearson correlation coefficients of 0.9–1, 0.7–0.89, 0.5–0.69, 0.26–0.49, and 0–0.25 between the two variables indicate very good, good, moderate, weak, and very weak correlations, respectively.

In general, high temperatures tend to increase the dissolution quantities of certain ions, such as K^{+}, Na^{+}, Cl^{-}, and SiO_2 (Zhu and Yu, 1995; Edmunds et al., 2006; Sung et al., 2012). However, in this study, there was a weak and wery weakly correlation between the water temperature and the other parameters (EC, K^{+}, Mg^{2+}, Na^{+}, and Cl^{-}); the absolute value of the correlation coefficient was usually less than 0.4. These results are consistent with those of previous studies. Rakib et al. (2020), Altın et al. (2009), Yusuf et al. (2013) found that the water temperature was very weakly correlated with other water quality parameters

Table 4. Statistical summary of the hydrochemical parameters of groundwater from the Göksu Plain (N = 24).

					Water quality guideline			
					Class			
Parameter	Mean	Max.	Min.	SD	I	II	III	IV
T (°C)	21.27	23.13	20.18	0.9	25	25	30	>30
pH	7.82	8.19	7.50	0.2	6.5–8.5	6.5–8.5	6.0–9.0	<6.0–9.0<
EC (µS/cm)	1471.74	5677.50	265.57	1289.9				
TDS (mg/L)	807.88	3941.30	156.61	839.66	500	1500	5000	>5000
Ca^{2+} (mg/L)	62.44	136.43	15.83	36.05	—	—	—	—
Mg^{2+} (mg/L)	39.53	125.64	13.40	26.79	—	—	—	—
K^{+} (mg/L)	9.42	34.46	2.41	8.65	—	—	—	—
Na^{+} (mg/L)	194.75	880.11	19.51	222.53	125	125	250	>250
Cl^{-} (mg/L)	284.22	1597.57	72.02	375.40	25	200	400	>400
SO_4^{2-} (mg/L)	195.97	321.53	105.61	64.83	200	200	400	>400
NO_3^{-} (mg/L)	12.49	13.34	12.06	0.36	5	10	20	>20
HCO_3^{-} (mg/L)	256.20	453.72	77.75	73.22	—	—	—	—
CO_3^{2-} (mg/L)	9.54	23.10	2.05	6.88	—	—	—	—
Ba (mg/L)	0.38	0.94	0.06	0.21	1	2	2	>2
Si (mg/L)	2.55	3.89	0.80	0.73	—	—	—	—
As (mg/L)	0.02	0.03	<LD	0.01				
B (mg/L)	0.81	1.72	0.41	0.3	—	—	—	—
SAR	5.13	17.41	0.45	4.97	—	—	—	—
RSC	−1.93	3.26	−13.16	3.73	—	—	—	—
%Na	47.59	86.27	10.71	24.60	—	—	—	—

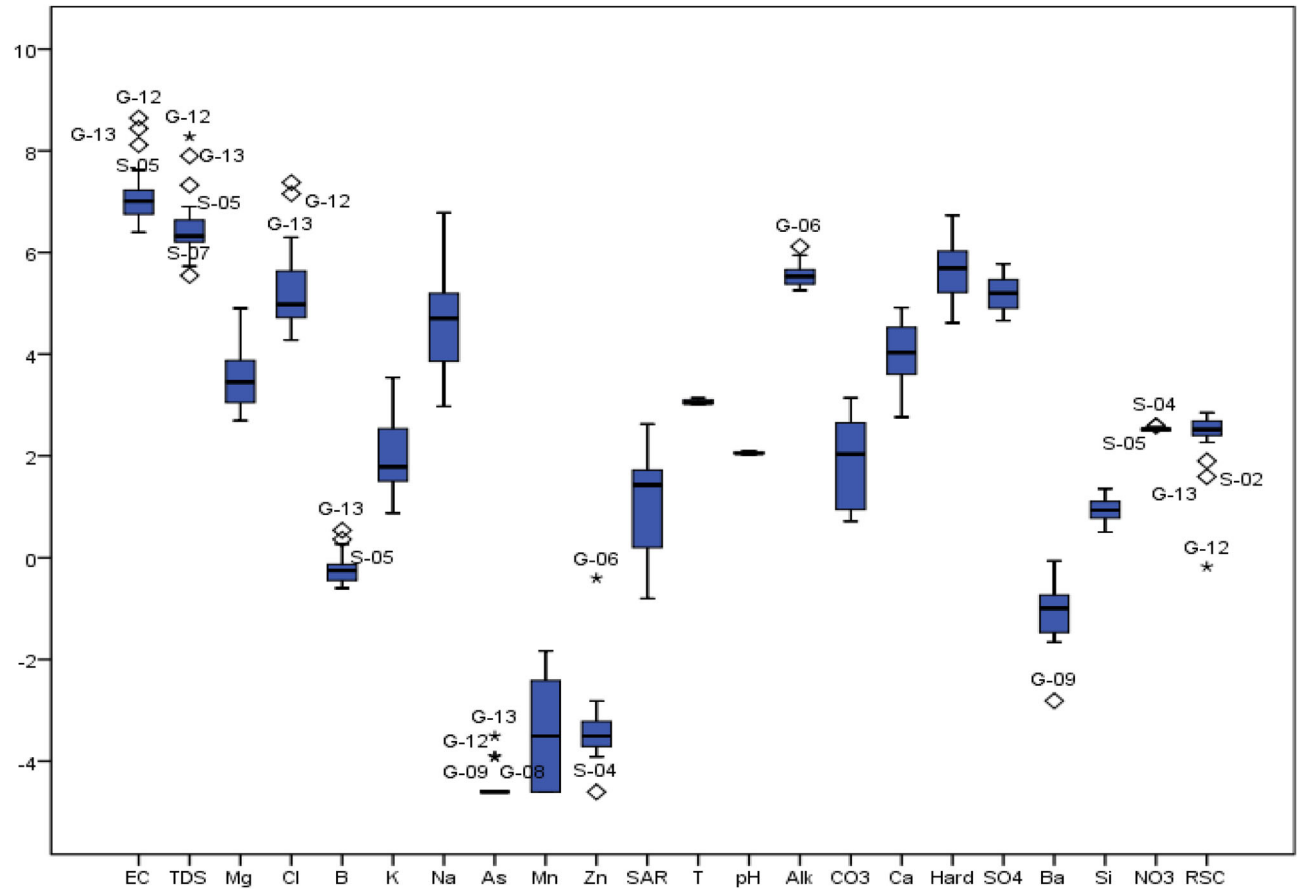


Figure 2. Box-and-whisker plots of variability in trace element concentrations in the water samples (EC, TDS, Cl^{-}, CO_3^{2-}, alkalinity, Ca^{2+}, Mg^{2+}, Hardness, K^{+}, Na^{+}, SO_4^{2-}, SAR, Ba, Si, and B, respectively).

such as alkalinity, EC, TOC, turbidity, total Kjeldahl nitrogen (TKN), DOC, salinity, and BOD5, which is similar to our findings.

The strong positive correlations between TDS, hardness, Ca^{2+}, and Mg^{2+} indicate that the bedrock was derived from the dissolution of carbonate and

Table 5. Correlation coefficient matrix of the chemical data for groundwater from the Göksu Plain (N = 24).

	EC	TDS	Mg^{2+}	Cl^{-}	B	K^{+}	Na^{+}	As	Mn	Zn	Sar	T	Ph	Alk	CO_3^{2-}	Ca^{2+}	Hard	SO_4^{2-}	Ba	Si	NO_3^{-}	RSC
EC	1																					
TDS	0.969**	1																				
Mg^{2+}	0.602**	0.683**	1																			
Cl^{-}	0.872**	0.884**	0.590**	1																		
B	0.904**	0.891**	0.515*	0.740**	1																	
K^{+}	0.725**	0.750**	0.387	0.638**	0.835**	1																
Na^{+}	0.591**	0.582**	0.157	0.732**	0.607**	0.702**	1															
As	0.566**	0.575**	0.345	0.559**	0.627**	0.682**	0.534**	1														
Mn	0.304	0.302	0.420*	0.220	0.316	0.082	0.054	0.052	1													
Zn	−0.092	0.003	0.127	−0.212	−0.027	0.093	−0.175	−0.120	0.200	1												
Sar	0.439*	0.406*	−0.099	0.579**	0.488*	0.620**	0.964**	0.472*	−0.040	−0.205	1											
T	0.348	0.376	0.258	0.375	0.230	0.370	0.168	0.151	0.071	0.254	0.093	1										
Ph	−0.026	−0.091	−0.251	−0.012	0.159	0.303	0.322	0.146	−0.433*	−0.306	0.410*	−0.316	1									
Alk	0.382	0.371	0.327	−0.018	0.412*	0.168	−0.298	−0.198	0.258	0.366	−0.371	0.045	−0.277	1								
CO_3^{2-}	−0.203	−0.273	−0.403	−0.128	−0.022	0.082	0.173	0.004	−0.410*	−0.358	0.295	−0.382	0.923**	−0.370	1							
Ca^{2+}	0.223	0.331	0.742**	0.227	0.084	−0.064	−0.239	−0.009	0.257	0.148	−0.472*	0.247	−0.512*	0.220	−0.548**	1						
Hard	0.431*	0.531**	0.926**	0.426*	0.307	0.165	−0.053	0.170	0.339	0.147	−0.314	0.271	−0.410*	0.292	−0.508*	0.938**	1					
SO_4^{2-}	0.251	0.350	0.402	0.255	0.309	0.466*	0.415*	0.077	0.018	0.156	0.292	0.219	−0.041	0.098	−0.175	0.364	0.417*	1				
Ba	0.273	0.270	0.502*	0.174	0.180	−0.135	−0.208	−0.207	0.701**	0.097	−0.348	0.171	−0.505*	0.338	−0.488*	0.574**	0.566**	0.035	1			
Si	0.438*	0.328	0.040	0.136	0.507*	0.351	0.029	0.033	0.101	−0.009	0.053	−0.163	0.366	0.612**	0.325	−0.325	−0.160	−0.204	−0.040	1		
NO_3^{-}	0.387	0.281	0.127	0.443*	0.290	0.087	0.184	0.027	0.302	−0.386	0.152	0.427*	0.066	−0.104	0.088	0.059	0.086	−0.204	0.460*	0.111	1	
RSC	0.096	0.031	−0.721*	0.332	0.017	0.032	0.470	0.187	−0.699	−0.594	0.658	−0.522	0.362	−0.383	0.613	−0.880**	−0.859**	−0.146	−0.503	0.497	−0.090	1

*Correlation is significant at the 0.05 level (2-tailed). ** Correlation is significant at the 0.01 level (2-tailed).

dolomite (Aiuppa et al., 2003; Jiang et al., 2009; Qin et al., 2013). Similar to the results of this study, Qin et al. (2013) reported relatively weak positive correlations between HCO_3^{-}, Ca^{2+}, and Mg^{2+}, which were due to the lamination and heterogeneous distribution of carbonate rock and dolostone around the sampling areas. Additionally, the strong positive correlation between TDS and Na^{+} and Cl^{-} can be interpreted as paleo-seawater intrusion, and an important factor in the assessment of groundwater chemistry is the storage of minerals with precipitation/evaporation properties (Rakib et al., 2020; Sae-Ju et al., 2020).

The correlation matrix analysis showed that there was very good correlation between Na^{+} and K^{+} (0.702). This positive correlation may indicate that these ions in the groundwater originated from the same sources. The reason that Na^{+} and K^{+} are introduced into grassland, forest, and cultivated land is due to the use of fertilizers for agricultural activities and anthropogenic causes, such as wastewater discharge from residential areas.

The EC of water depends on the total concentration, mobility, valence, and temperature of the ions. The EC of water increases as T increases, and the concentration of the ions in the water increases. In this study, there was a weak correlation between EC and T (0.348). Therefore, the EC value is a good indicator of the total ion concentration in water. Accordingly, the EC represents a qualitative estimate of inorganic pollution. Information on TDS can be considered a good indicator of pollution. The EC was positively correlated with water salinity, ions such as Cl^{-}, Mg^{2+}, B, K^{+}, Na^{+}, Si, and parameters such as SAR, hardness, and TDS (see Table 5). The high correlation implies that groundwater chemistry in the study area was mainly controlled by these parameters. In addition, this correlation may be considered as due to the influence of seawater intrusion. Similarly, the strong correlation between Na^{+} and Cl^{-} and that between Na^{+} and B may be interpreted as a result of seawater intrusion. Water containing Na^{+} and Cl^{-} ions in high concentrations is characterized as saline water, whereas water containing relatively high Ca^{2+} and HCO_3^{-} concentrations in addition to other major ions is characterized as freshwater (Appelo and Postma, 2005; Sae-Ju et al., 2020). Na^{+} and Cl^{-} were the dominant ions in areas close to the coast. The strong correlation between Na^{+} and Cl^{-} showed the effect of seawater–groundwater mixing. As shown in the correlation matrix, K^{+} can be considered as it is also associated with seawater intrusion and it has a positive correlation with B and Cl^{-}. Because seawater intrusion is the result of cation exchange, the Ca^{2+}

concentration was lower than that of Na^+ in the groundwater where the seawater intruded.

According to the correlation coefficient matrix, there was a weak correlation between Si and pH, which may indicate that silicate mineral weathering processes are related to increases in pH. This conclusion is supported by the statistical and graphical methods and hydrochemical analyses performed in 23 wells in the Shagari area by Owoseni et al. (2013).

The variance explanation rates of the hydrochemical components are listed in Table 6. For example, it indicates that 95% of the variable TDS is explained by the PCs. Here, variables with low common variance (below 0.50) were excluded from the analysis and FA was re-performed. In this case, both the KMO value and the value of the variance explanation statistic reached higher values. Accordingly, T and Mn components were excluded from the analysis and when the analysis was repeated, the variance explanation rate for all variables in the analysis was greater than 0.5.

In this study, FA was applied to detect the parameters that primarily contributed to the changes in water quality. While determining the number of PCs to be rotated, one of the methods other than eigenvalue statistics is the scree plot (Figure 3). In this graph, the number of PCs determined by the point at which the slope begins to disappear is determined. Accordingly, four PCs were identified.

Table 6. Variance explanation rates using PCA for hydrochemical data from the Göksu Plain.

	Initial	Extraction		Initial	Extraction		Initial	Extraction
EC	1	.94	As	1	.50	CO_3^{2-}	1	.68
TDS	1	.95	Mn	1	**.48**	Ca^{2+}	1	.81
Mg^{2+}	1	.79	Zn	1	.52	Hardness	1	.83
Cl^-	1	.90	SAR	1	.83	SO_4^{2-}	1	.56
B	1	.94	T	1	**.26**	Ba	1	.81
K^+	1	.89	pH	1	.67	Si	1	.91
Na^+	1	.87	Alk	1	.92	NO_3^-	1	.83
RSC	1	.77						

Extraction method: principal component analysis. The bold values indicate variables with low common variance (below 0.50).

The high correlation between NO_3^- and T may be associated with pollution that occurred as a result of intense agricultural activities in the surrounding region. The groundwater quality in the areas surrounding Kayseri agricultural activities demonstrated high concentrations of NO_3^- and NaCl that caused contamination due to untreated sewage and agricultural waste during spring (Elhatip et al., 2003; Baba and Ayyildiz, 2006).

Although Re et al. (2013) and El Yaouti et al. (2009) detected relatively low Cl concentrations in their underground water studies; they noted that there was extremely high enrichment of NO_3^- ions. The samples from our study could be affected by the input of manure-derived NO_3^- or septic effluents. Alternatively, high Cl^- and low NO_3^- contents were measured in a specific area of the aquifer and were attributed to seawater intrusion. It was observed that there was statistically moderate correlation ($r = 0.443$) between the changes in the Cl^- and NO_3^- contents measured in the wells throughout the year in the study conducted in the Göksu Plain.

For the scree plot and eigenvalues greater than or equal to 1, four PCs were selected that explained 80.22% of the total variance of the data set. The parameter loadings for the four PCs from the FA are presented in Table 7, and those marked in bold are considered strong values. The terms strong, moderate,

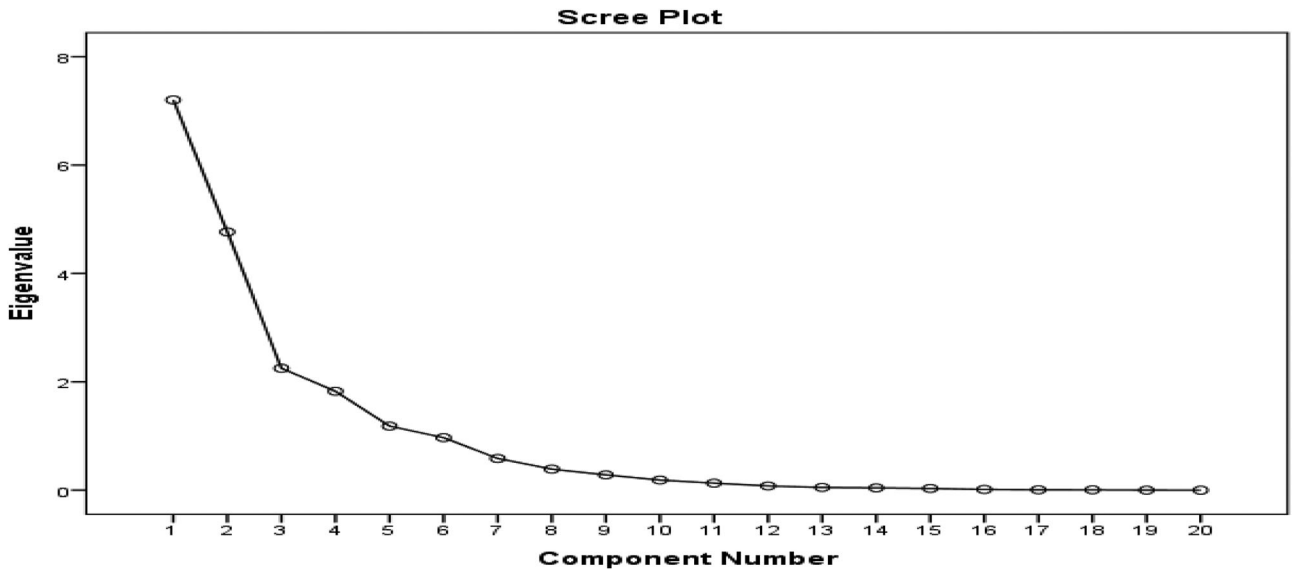


Figure 3. Scree plot of eigenvalues using the principal components for the hydrochemical data from the Göksu Plain.

Table 7. Varimax rotated factor matrix for hydrochemical data from the Göksu Plain.

	PC			
	1	2	3	4
K^+	**0.899**	−0.097	0.211	−0.172
Na^+	**0.874**	−0.254	−0.254	0.042
Cl^-	**0.860**	0.252	−0.017	0.324
TDS	**0.847**	0.363	0.311	0.103
B	**0.844**	0.088	0.454	0.104
EC	**0.825**	0.268	0.382	0.229
SAR	**0.756**	−0.475	−0.263	0.040
As	**0.708**	−0.009	−0.023	0.001
SO_4^{2-}	**0.474**	0.269	−0.197	−0.473
Ca^{2+}	0.034	**0.918**	−0.073	−0.020
Hard	0.269	**0.892**	0.030	−0.016
CO_3^{2-}	0.042	**−0.777**	−0.027	0.244
Mg^{2+}	0.487	**0.749**	0.140	0.011
pH	0.242	**−0.743**	0.026	0.152
Ba	−0.082	**0.728**	0.230	0.374
RSC	−0.601	**−0.613**	0.245	−0.031
Alk	−0.003	0.314	**0.885**	−0.233
Si	0.205	−0.314	**0.862**	0.129
NO_3^-	0.173	0.101	0.080	**0.857**
Zn	−0.104	0.221	0.270	**−0.682**
Eigenvalues	6.539	5.164	2.410	1.931
Total % of Vaiance	32.694	25.821	12.050	9.657
Cumulative %	32.694	58.515	70.565	80.222

The bold values indicate PCs to which hydrochemical parameters in terms of loading scores.

Table 8. Component score covariance matrix.

Component	1	2	3	4
1	1.000	0.000	0.000	0.000
2	0.000	1.000	0.000	0.000
3	0.000	0.000	1.000	0.000
4	0.000	0.000	0.000	1.000

Extraction method: principal component analysis. Rotation method: Varimax with Kaiser Normalization. Component Scores.

Table 9. Component score coefficient matrix.

	Component			
	1	2	3	4
EC	0.102	0.024	0.122	0.084
TDS	0.113	0.042	0.088	0.018
Mg^{2+}	0.054	0.134	0.014	−0.001
Cl^-	0.119	0.037	−0.052	0.135
B	0.114	−0.019	0.160	0.011
K^+	0.153	−0.057	0.061	−0.144
Na^+	0.160	−0.065	−0.135	−0.030
As	0.119	−0.020	−0.037	−0.038
Zn	0.003	0.019	0.116	−0.356
SAR	0.147	−0.107	−0.126	−0.030
pH	0.052	−0.155	0.029	0.048
Alk	−0.031	0.025	0.374	−0.121
CO_3^{2-}	0.016	−0.151	0.014	0.108
Ca^{2+}	−0.016	0.188	−0.067	0.013
Hard	0.020	0.172	−0.031	0.001
SO_4^{2-}	0.104	0.036	−0.112	−0.271
Ba	−0.063	0.152	0.074	0.224
Si	0.002	−0.098	0.377	0.045
NO_3^-	−0.023	0.036	0.020	0.454
RSC	−0.091	−0.118	0.153	−0.002

and weak, which were applied to the factor loadings, refer to the absolute loading values of >0.75, 0.75–0.5, and 0.5–0.3, respectively. From Table 7, it can be seen that the first PC (PC1) shows a strong and positive correlation with K (0.899), Na^+ (0.874), Cl^- (0.860), TDS (0.847), B (0.844), EC (0.825), and SAR (0.756), a moderate positive correlation with As (0.708), and a weak positive correlation with SO_4^{2-} (0.474); these variables explain 32.694% of the total variance. The second PC explained 25.821% of the total variance, while having a strong positive relationship with Ca^{2+}, hardness, and Mg^{2+}, and a moderate positive relationship with Ba. It has a strong negative relationship with CO_3^{2-}, and a moderate negative relationship with pH and RSC. Three PCs explained 70.565% of the variance, and PC3 is correlated with Alk and Si with a high positive degree. The variance explanation rate of the last PC (PC4), which was positive for NO_3^- and negative for Zn, was 9.657%.

According to the results in Table 8, the fact that the covariance values are zero provides the assumption that the factors are unrelated. The factor scores in the component column in Table 9 have a normal distribution and do not have multicollinearity problems. The obtained factor scores can be used as variables in other analyses.

It is well known that hardness is correlated with Ca^{2+} and Mg^{2+} contents (Reghunath et al., 2002; Papatheodorou et al., 2006). This factor accounted for the temporary water hardness. Additionally, the presence of rocks, such as carbonate and dolostone around the sampling areas, can be attributed to the dissolution of soil and minerals. pH and CO_3^{2-} are two important variables controlled by natural processes.

Several different studies have shown that the source of nitrate pollution may be the result of different agricultural practices and hydrogeological structures of a region (Kim et al., 2005; Grassi et al., 2007; Stigter et al., 2008; Zhao et al., 2010; Landon et al., 2011; Güler et al., 2012; Qin et al., 2013). Rekha et al. (2011) characterized the leaching of NO_3–N into shallow groundwater from agricultural fields under different cultivation practices. Taking into consideration the intensive agricultural activities in this area and the commercial composites that have been applied for a long period of time, the high score of PC4 may be due to agricultural fertilizers. In an area similar to our study area (Figure 4) (a landscape with intensive agriculture, close to the sea and river), Kim et al. (2005) reported that under toxic conditions, the main component of fertilizers, NH_4^+, is easily oxidized into NO_3^- by nitrification. These authors stated that the part that constituted 6.3% of the total variance was primarily associated with a high positive loading for

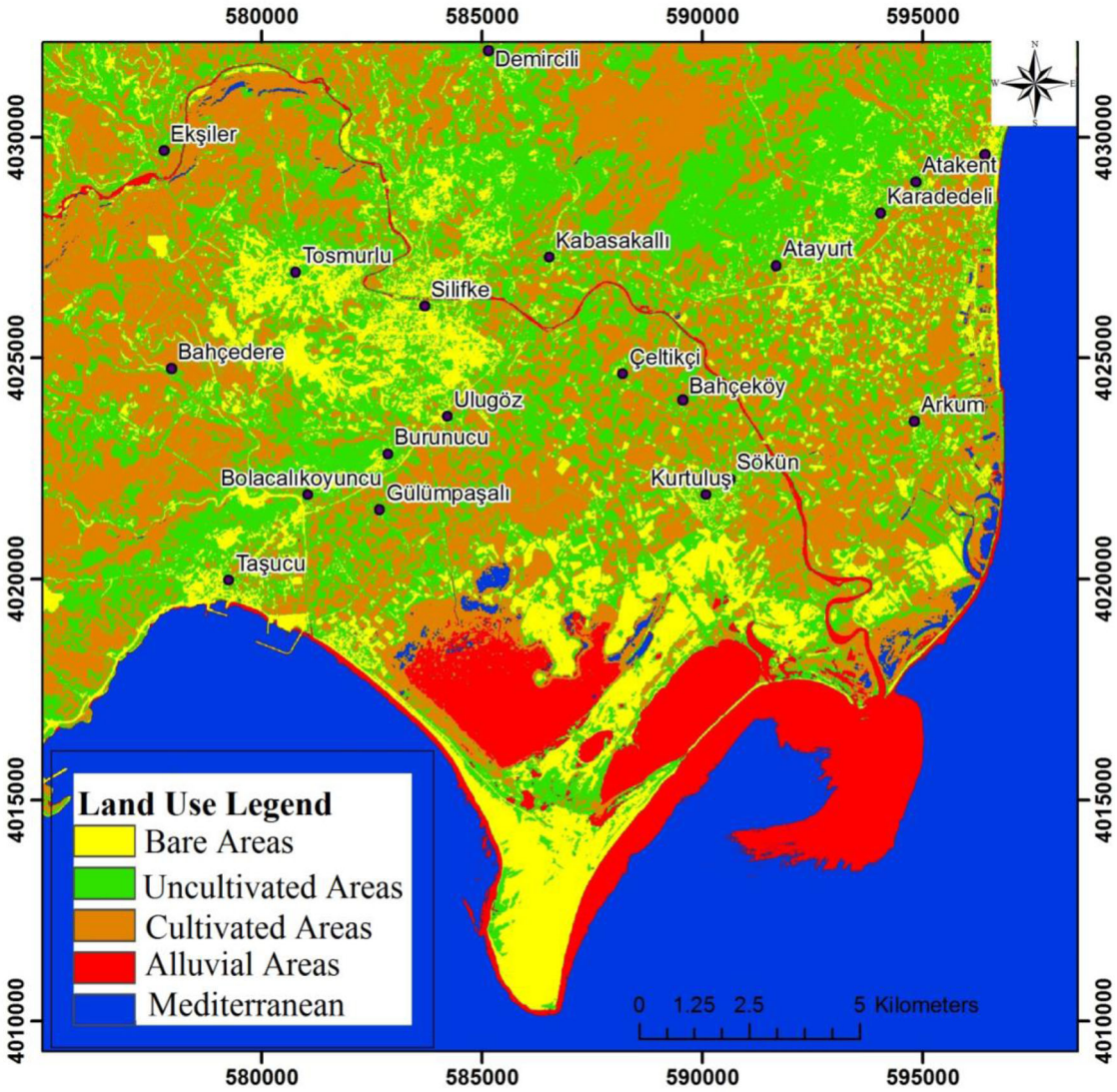


Figure 4. A map of land use in the Göksu Plain. Source: Güner, 2016.

NO_3^- and negative moderate loadings for pH and HCO_3^-.

Ba is present as a trace element in both igneous and sedimentary rocks. This element is not found in a free form in nature and occurs in a number of compounds, most commonly in the form of barite ($BaSO_4$) and, to a lesser extent, witherite ($BaCO_3$). The acetate, nitrate, and salts of barium are soluble in water, but the carbonate, chromate, fluoride, oxalate, phosphate, and sulfate salts are quite insoluble. The aqueous solubility of barium compounds increases as the pH decreases. The concentration of barium ions in natural aquatic systems will be limited by naturally occurring anions, such as sulfates and carbonates, and by the possible adsorption of barium ions onto metal oxides and hydroxides. Barium can only reach toxic concentrations if the water contains a low concentration of sulfate.

It has been stated that the primary reason for nitrate intrusion into shallow water is the fertilizer used to increase crop productivity (Krapac et al., 2002; Psychoyou et al., 2007; Jalali, 2011). The wetland of the Göksu Plain has a particularly high amount of green vegetable production.

Two separate dendrograms were created for the water quality parameters considered and the hydrochemical sampling sites (Figure 5). The clusters are obtained using Ward's method with Euclid's metric of the square. From Figure 5, according to the CA, two major clusters are identified for the measured water quality parameters. In Figure 5, it is clear that the first cluster contained pH, NO_3^-, RSC, T, K^+, CO_3^{2-},

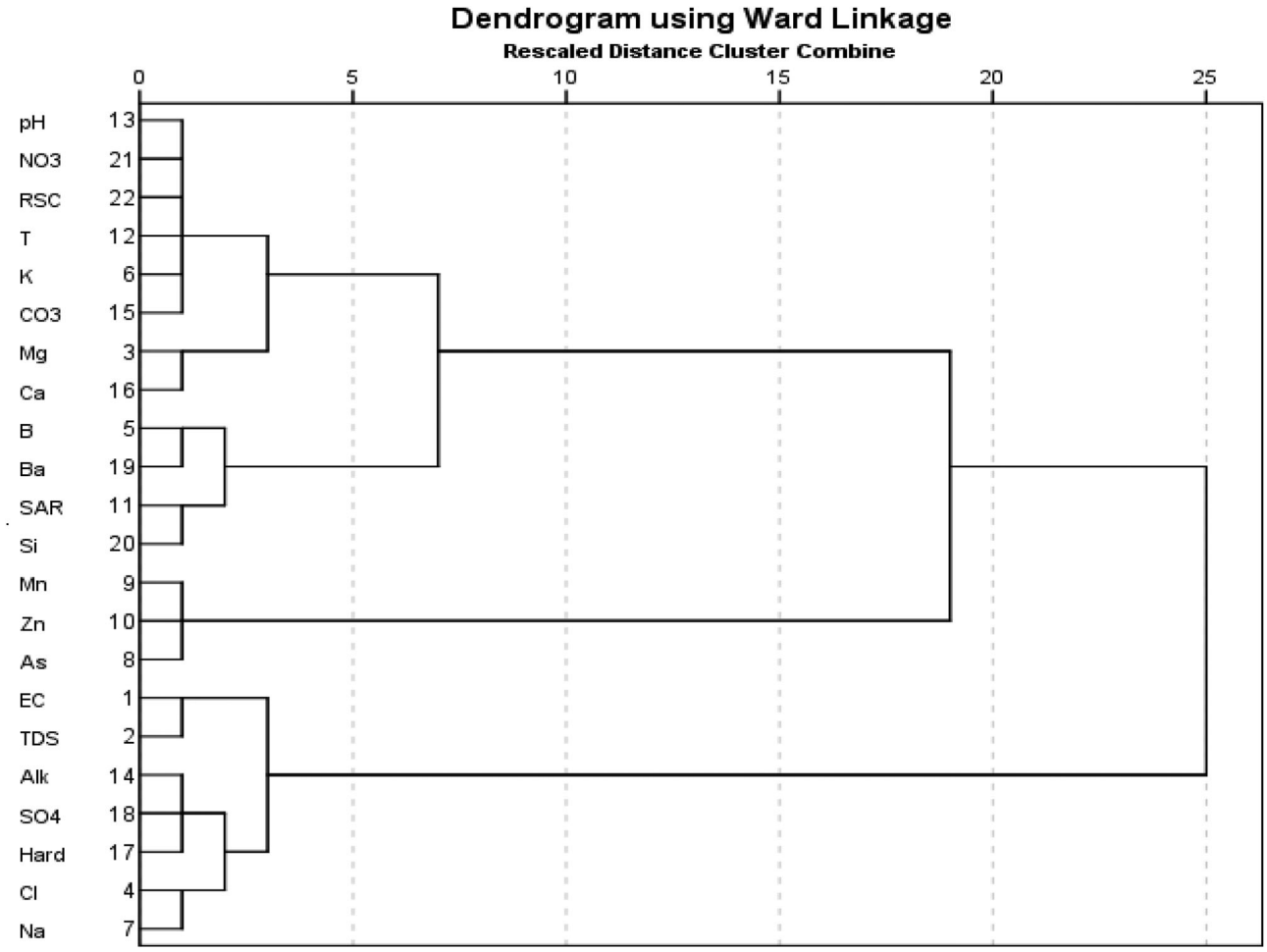


Figure 5. A dendrogram showing the water quality parameters of the Göksu Plain (y-axis).

Table 10. Geochemical criteria for distinguishing the origin of saltwater.

Measurement	Criteria
Na/Cl ratio	=0.86 seawater <0.86 seawater intrusion >1.0 anthropogenic sources (e.g., sewage)
Ca/Mg	>1.0 seawater intrusion
$Ca/(HCO_3 + SO_4)$	>1.0 seawater intrusion

Mg^{2+}, Ca^{2+}, B, Ba, SAR, Si, Mn, Zn, and As, and the second cluster contained EC, TDS, alkalinity, SO_4^{2-}, hardness, Cl^-, and Na^+.

To distinguish the seawater intrusion from the other salinity resources in coastal aquifers, the geochemical ratios of Na/Cl (a limit of 0.86), Ca/Mg (a limit of 1.00), and $Ca/(HCO_3+SO_4)$ (a limit of 1.00) have been used (Al-Khatib and Al-Najar, 2011; Sherif et al., 2011; Re et al., 2013) (Table 10). The values of the geochemical ratios calculated for this study are shown in Figure 6. In general, freshwater was dominated by calcium, and seawater was dominated by magnesium. The Ca/Mg ratio provided an indicator of the contaminated seawater–freshwater interface. The Ca/Mg ratios in the G-01, G-02, G-03, G-04, S-01, S-02, S-06, S-07, S-08, S-09, S-10, and S-11 wells were higher because Mg^{2+} was considerably more abundant than Ca^{2+} (Figure 6).

According to the values in Table 10 and Figure 6, the Na/Cl ratios of the G-01, G-03, G-12, S-01, S-02, S-03, S-07, S-09, and S-11 wells implied greater seawater intrusion compared to the other sampling wells. In addition, the other sampling stations were slightly below the 1:1 line in the Na/Cl plot, indicating the absence of clear geochemical evidence of seawater intrusion. It should be noted that the G-01, G-03, S-01, S-02, and S-03 wells are closer to the Göksu River, and the other wells (G-12, S-07, S-09, and S-11) may show that seawater intrusion has extended inland. The Ca/Mg ratio may indicate the possibility of greater seawater intrusion than on the Silifke side.

The SAR ratio is an important reference for the classification of water regarding the salinity effect. Most of the samples were in the best class for the SAR ratio. In contrast to the general trend of the sampling area, the G-05, G-11, G-12, S-05, and S-06 wells

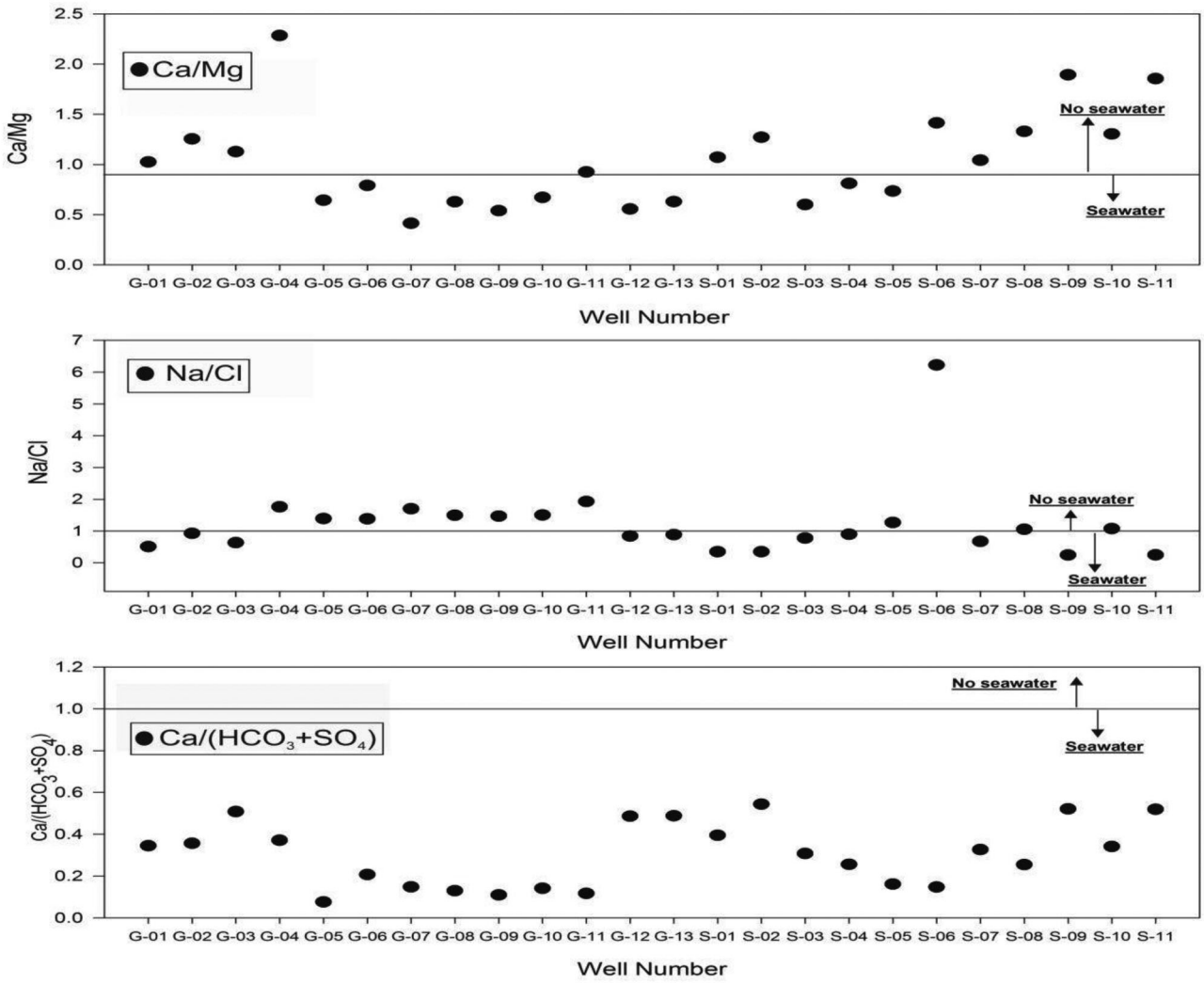


Figure 6. Geochemical ratios for 24 wells.

Table 11. Classification of water according to the %Na value (Sahinci, 1991).

%Na	Irrigation water classification
<20	Very well
20–40	Well
40–60	Good
60–80	Questionable use

were higher than the SAR ratio of 12, which can cause serious physical problems and difficulties for plants to absorb water.

It has been concluded from studies that water consistently containing more than 2.5 meq/L sodium carbonate is unsuitable for irrigation. Water with RSC values ranging from 1.25 to 2.5 meq/L or less than 1.25 meq/L can be used safely using a proper grading system. Water with values higher than 2.5 meq/L is not suitable for irrigation. Because wells with a negative RSC value do not cause any problems, the RSC value of these wells is assumed to be zero (Lloyd and Heathcote, 1985). According to the values presented in Table 4, based on the RSC, only G-05 Class II is suitable for irrigation, and the other samples are first-class irrigation water. The %Na value is an important parameter for groundwater, which indicates whether the water is suitable for use as irrigation water in agricultural areas.

According to the classification provided in Table 11, the maximum %Na value was identified at the G-05 sampling point in the study area of Göksu, which was classified as "not suitable." The other sampling points were classified as "questionable use" (G-04, G-07, G-08, G-09, G-10, G-11, G-12, G-13, S-03, S-04, S-05, S-08, and S-10), "good" (G-02, G-03, G-06, and S-07), and "well" (G-01, S-01, S-02, S-09, and S-11).

Conclusions

This study has demonstrated that multivariate statistical techniques are useful for water quality assessment and investigation of salinity in coastal aquifers near wetland

areas. A total of 24 artesian well water samples were collected between May 2010 and April 2011 from the Göksu Plain, which is one of the coastal aquifers located on the Turkish Mediterranean coast. In the assessment of groundwater for salinity, TDS can be used, which is calculated as the sum of the major ions. None of the water samples collected from the sampling points in the Göksu Plain were classified as freshwater (TDS <500 mg/L), and all of the points were considered as brackish water (Custodio and Llamas, 1976). As an increase in the salinity of groundwater in coastal areas reveals the presence of saline water intrusion, the quality of freshwater aquifers is reduced for their usage for irrigation.

It has been determined that the potential cause of salinity in coastal aquifer systems and seawater intrusion is due to an increase in the concentrations of Na^+, Mg^{2+}, Ca^{2+}, and HCO_3^-. The presence of NO_3^-, which, together with seawater intrusion, represents an issue for groundwater management in the region, may depend on the use of fertilizers. FA and correlation analysis grouped the 24 stations into four clusters with similar characteristics based on each factor obtained by FA. The statistical results of FA indicate that the high factor loadings of EC, Na^+, K^+, Cl^-, and TDS typically originate from marine sources, seawater intrusion into aquifers, or distribution from marine aerosols in rainfall. The results of the cluster analysis demonstrated that the groundwater quality was affected by seawater intrusion (Na^+, Cl^-).

For the assessment of the origin of groundwater, the Na/Cl, Ca/Mg, and Ca/(HCO_3+SO_4) values were measured. These results may indicate that seawater intrusion causes a change in the water quality of the area. In addition, according to the SAR, %Na, and RSC analyses results, the use of underground water for irrigation is an important factor affecting salinization.

A comprehensive groundwater monitoring system and protection and control systems should be established in such a valuable wetland area. Thus, actual data can be obtained from this system. In this way, more comprehensive suggestions can be made for further research. In future studies, methods that include deep learning and algorithms using large data sets may be preferred for classification, feature selection and extraction. Among these methods that have been used frequently in recent years, one of the methods such as decision tree (DT), k-nearest neighbors (KNN), support vector machines (SVM) and artificial neural networks (ANN) can be chosen for future analysis.

Acknowledgment

The authors thank Cukurova University for their support.

ORCID

Esra Deniz Güner http://orcid.org/0000-0002-0492-2999

References

Aiuppa, A., Bellomo, S., Brusca, L., D'Alessandro, W., and Federico, C. 2003. Natural and anthropogenic factors affecting groundwater quality of an active volcano (Mt. Etna, Italy). *Applied Geochemistry* 18(6):863–882.

Al-Khatib, M., and Al-Najar, H. 2011. Hydro-geochemical characteristics of groundwater beneath the Gaza Strip. *Journal of Water Resource and Protection* 335043(5): 341–348.

Altın, A., Filiz, Z., and Filik Iscen, C. 2009. Assessment of seasonal variations of surface water quality characteristics for Porsuk Stream. *Environmental Monitoring and Assessment* 158(1–4):51–65.

Anonymous. 1988. Turkish Water Pollution Control Regulation. Official Gazette 19919.

Appelo, C. A. J., and Postma, D. 2005. *Geochemistry, Groundwater and Pollution*. Boca Raton, FL: CRC Press.

Arslan, H. 2013. Application of multivariate statistical techniques in the assessment of groundwater quality in seawater intrusion area in Bafra Plain, Turkey. *Environmental Monitoring and Assessment* 185(3): 2439–2452.

Baba, A., and Ayyildiz, O. 2006. Urban groundwater pollution in turkey. In *Urban Groundwater Management and Sustainability*, eds. Tellam, J. H., Rivett, M. O., Israfilov, R. G., and Herringshaw, L. G. Basel, Switzerland: Springer, 93–110.

Belkhiri, L., and Narany, T. S. 2015. Using multivariate statistical analysis, geostatistical techniques and structural equation modeling to identify spatial variability of groundwater quality. *Water Resources Management* 29(6): 2073–2089.

Bhuiyan, M. A., Rakib, M. A., Dampare, S. B., Ganyaglo, S., and Suzuki, S. 2011. Surface water quality assessment in the central part of Bangladesh using multivariate analysis. *KSCE Journal of Civil Engineering* 15(6):995–1003.

Busico, G., Kazakis, N., Cuoco, E., Colombani, N., Tedesco, D., Voudouris, K., et al. 2020. A novel hybrid method of specific vulnerability to anthropogenic pollution using multivariate statistical and regression analyses. *Water Research* 171:115386.

Cai, H., Savenije, H. H., Zuo, S., Jiang, C., and Chua, V. P. 2015. A predictive model for salt intrusion in estuaries applied to the Yangtze estuary. *Journal of Hydrology* 529: 1336–1349.

Cheng, X.-J., Zhan, W., Guo, Z.-R., and Yuan, L.-R. 2012. A modeling study on saltwater intrusion to western four watercourses in the Pearl River estuary. *China Ocean Engineering* 26(4):575–590.

Custodio, E., and Llamas, M. R. 1976. *Hidrología subterránea [Groundwater hydrology]*. Vol. 2. Barcelona, Spain: Editorial Omega.

De Stefano, L., Fornés, J. M., López-Geta, J. A., and Villarroya, F. 2015. Groundwater use in Spain: An overview in light of the EU Water Framework Directive. *International Journal of Water Resources Development* 31(4):640–656.

Demirel, Z. 2007. Monitoring of heavy metal pollution of groundwater in a phreatic aquifer in Mersin-Turkey. *Environmental Monitoring and Assessment* 132(1–3): 15–23.

Dragon, K., and Gorski, J. 2015. Identification of groundwater chemistry origins in a regional aquifer system (Wielkopolska region, Poland). *Environmental Earth Sciences* 73(5):2153–2167.

Eaton, F. M. 1950. Significance of carbonates in irrigation waters. *Soil Science* 69(2):123–134.

Edmunds, W. M., Ma, J., Aeschbach-Hertig, W., Kipfer, R., and Darbyshire, D. P. F. 2006. Groundwater recharge history and hydrogeochemical evolution in the Minqin Basin, North West China. *Applied Geochemistry* 21(12): 2148–2170.

Eissa, M. A., Mahmoud, H. H., Shouakar-Stash, O., El-Shiekh, A., and Parker, B. 2016. Geophysical and geochemical studies to delineate seawater intrusion in Bagoush area, Northwestern coast, Egypt. *Journal of African Earth Sciences* 121:365–381.

El Yaouti, F., El Mandour, A., Khattach, D., Benavente, J., and Kaufmann, O. 2009. Salinization processes in the unconfined aquifer of Bou-Areg (NE Morocco): A geostatistical, geochemical, and tomographic study. *Applied Geochemistry* 24(1):16–31.

Elhatip, H., Afşin, M., Dirik, K., Kurmaç, Y., and Kavurmacı, M. 2003. Influences of human activities and agriculture on groundwater quality of Kayseri-Incesu-Dokuzpınar springs, central Anatolian part of Turkey. *Environmental Geology* 44(4):490–494.

Fadili, A., Najib, S., Mehdi, K., Riss, J., Malaurent, P., and Makan, A. 2017. Geoelectrical and hydrochemical study for the assessment of seawater intrusion evolution in coastal aquifers of Oualidia, Morocco. *Journal of Applied Geophysics* 146:178–187.

Giardino, C., Brando, V. E., Dekker, A. G., Strömbeck, N., and Candiani, G. 2007. Assessment of water quality in Lake Garda (Italy) using Hyperion. *Remote Sensing of Environment* 109(2):183–195.

Gong, W., and Shen, J. 2011. The response of salt intrusion to changes in river discharge and tidal mixing during the dry season in the Modaomen Estuary, China. *Continental Shelf Research* 31(7–8):769–788.

Grassi, S., Cortecci, G., and Squarci, P. 2007. Groundwater resource degradation in coastal plains: The example of the Cecina area (Tuscany–Central Italy). *Applied Geochemistry* 22(11):2273–2289.

Güler, C., Kurt, M. A., Alpaslan, M., and Akbulut, C. 2012. Assessment of the impact of anthropogenic activities on the groundwater hydrology and chemistry in Tarsus coastal plain (Mersin, SE Turkey) using fuzzy clustering, multivariate statistics and GIS techniques. *Journal of Hydrology* 414:435–451.

Güner, E. D., 2016. *Determination of groundwater quality and distribution levels in Göksu Delta*, PhD diss., University of Çukurova.

Güner, E. D., Tekin, S., and Seçkin, G. 2018. An assessment of shallow groundwater wells in an agricultural and coastal area in Göksu Delta, Turkey. *Bilge International Journal of Science and Technology Research* 2(1):9–16.

Hounsinou, S. P. 2020. Assessment of potential seawater intrusion in a coastal aquifer system at Abomey - Calavi, Benin. *Heliyon* 6(2):e03173.

Huang, W., Hagen, S., Bacopoulos, P., and Wang, D. 2015. Hydrodynamic modeling and analysis of sea-level rise impacts on salinity for oyster growth in Apalachicola Bay, Florida. *Estuarine, Coastal and Shelf Science* 156: 7–18.

Jalali, M. 2011. Nitrate pollution of groundwater in Toyserkan, western Iran. *Environmental Earth Sciences* 62(5):907–913.

Jeong, S., Yeon, K., Hur, Y., and Oh, K. 2010. Salinity intrusion characteristics analysis using EFDC model in the downstream of Geum River. *Journal of Environmental Sciences* 22(6):934–939.

Jiang, Y., Wu, Y., Groves, C., Yuan, D., and Kambesis, P. 2009. Natural and anthropogenic factors affecting the groundwater quality in the Nandong karst underground river system in Yunan, China. *Journal of Contaminant Hydrology* 109(1–4):49–61.

Kang, M., and Jackson, R. B. 2016. Salinity of deep groundwater in California: Water quantity, quality, and protection. *Proceedings of the National Academy of Sciences* 113(28):7768–7773.

Kazakis, N., Pavlou, A., Vargemezis, G., Voudouris, K. S., Soulios, G., Pliakas, F., et al. 2016. Seawater intrusion mapping using electrical resistivity tomography and hydrochemical data. An application in the coastal area of eastern Thermaikos Gulf, Greece. *The Science of the Total Environment* 543:373–387.

Kim, J.-H., Kim, R.-H., Lee, J., Cheong, T.-J., Yum, B.-W., and Chang, H.-W. 2005. Multivariate statistical analysis to identify the major factors governing groundwater quality in the coastal area of Kimje, South Korea. *Hydrological Processes* 19(6):1261–1276.

Kim, K.-H., Yun, S.-T., Park, S.-S., Joo, Y., and Kim, T.-S. 2014. Model-based clustering of hydrochemical data to demarcate natural versus human impacts on bedrock groundwater quality in rural areas, South Korea. *Journal of Hydrology* 519:626–636.

Krapac, I. G., Dey, W. S., Roy, W. R., Smyth, C. A., Storment, E., Sargent, S. L., et al. 2002. Impacts of swine manure pits on groundwater quality. *Environmental Pollution* 120(2):475–492.

Landon, M. K., Green, C. T., Belitz, K., Singleton, M. J., and Esser, B. K. 2011. Relations of hydrogeologic factors, groundwater reduction-oxidation conditions, and temporal and spatial distributions of nitrate, Central-Eastside San Joaquin Valley, California, USA. *Hydrogeology Journal* 19(6):1203–1224.

Liu, B., Peng, S., Liao, Y., and Long, W. 2018. The causes and impacts of water resources crises in the Pearl River Delta. *Journal of Cleaner Production* 177:413–425.

Lloyd, J. W., and Heathcote, J. A. A. 1985. *Natural Inorganic Hydrochemistry in Relation to Ground Water*. Oak Ridge, TN: OSTI.

Machiwal, D., and Jha, M. K. 2015. Identifying sources of groundwater contamination in a hard-rock aquifer system using multivariate statistical analyses and GIS-based geostatistical modeling techniques. *Journal of Hydrology: Regional Studies* 4:80–110.

Magyar, N., Gábor Hatvani, I., Székely, I. K., Herzig, A., Dinka, M., and Kovács, J. 2013. Application of multivariate statistical methods in determining spatial changes in water quality in the Austrian part of Neusiedler See. *Ecological Engineering* 55:82–92.

Morgan, L. K., and Werner, A. D. 2015. A national inventory of seawater intrusion vulnerability for Australia. *Journal of Hydrology: Regional Studies* 4:686–698.

Moyo, N. A. G. 2013. An analysis of the chemical and microbiological quality of ground water from boreholes and shallow wells in Zimbabwe. *Physics and Chemistry of the Earth, Parts A/B/C* 66:27–32.

Najib, S., Fadili, A., Mehdi, K., Riss, J., and Makan, A. 2017. Contribution of hydrochemical and geoelectrical approaches to investigate salinization process and seawater intrusion in the coastal aquifers of Chaouia, Morocco. *Journal of Contaminant Hydrology* 198:24–36.

Owoseni, J. O., Tamarautobou, E. U., and Asiwaju-Bello, Y. A. 2013. Application of sequential analysis and geographic information systems for hydrochemical evolution survey, Shagari Environ, Southwestern Nigeria. *Amerikan International Journal of Contemporary Reserch* 3(3): 38–48.

Palma, P., Ledo, L., Soares, S., Barbosa, I. R., and Alvarenga, P. 2014. Spatial and temporal variability of the water and sediments quality in the Alqueva reservoir (Guadiana Basin; southern Portugal). *Science of the Total Environment* 470:780–790.

Papatheodorou, G., Demopoulou, G., and Lambrakis, N. 2006. A long-term study of temporal hydrochemical data in a shallow lake using multivariate statistical techniques. *Ecological Modelling* 193(3):759–776.

Psychoyou, M., Mimides, T., Rizos, S., and Sgoubopoulou, A. 2007. Groundwater hydrochemistry at Balkan coastal plains—The case of Marathon of Attica, Greece. *Desalination* 213(1):230–237.

Qi, H., Ma, C., He, Z., Hu, X., and Gao, L. 2019. Lithium and its isotopes as tracers of groundwater salinization: A study in the southern coastal plain of Laizhou Bay, China. *The Science of the Total Environment* 650: 878–890.

Qin, R., Wu, Y., Xu, Z., Xie, D., and Zhang, C. 2013. Assessing the impact of natural and anthropogenic activities on groundwater quality in coastal alluvial aquifers of the lower Liaohe River Plain, NE China. *Applied Geochemistry* 31:142–158.

Raghunath, H. M. 1987. *Ground Water*. New Delhi, India: New Age International.

Rakib, M. A., Sasaki, J., Matsuda, H., Quraishi, S. B., Mahmud, M. J., Bodrud-Doza, M., et al. 2020. Groundwater salinization and associated co-contamination risk increase severe drinking water vulnerabilities in the southwestern coast of Bangladesh. *Chemosphere* 246: 125646.

Re, V., Sacchi, E., Martin-Bordes, J. L., Aureli, A., El Hamouti, N., Bouchnan, R., et al. 2013. Processes affecting groundwater quality in arid zones: The case of the Bou-Areg coastal aquifer (North Morocco). *Applied Geochemistry* 34:181–198.

Reghunath, R., Murthy, T. S., and Raghavan, B. R. 2002. The utility of multivariate statistical techniques in hydrogeochemical studies: An example from Karnataka, India. *Water Research* 36(10):2437–2442.

Rekha, P. N., Kanwar, R. S., Nayak, A. K., Hoang, C. K., and Pederson, C. H. 2011. Nitrate leaching to shallow groundwater systems from agricultural fields with different management practices. *Journal of Environmental Monitoring* 13(9):2550–2558.

Ros, S. E. M., and Zuurbier, K. G. 2017. The impact of integrated aquifer storage and recovery and brackish water reverse osmosis (ASRRO) on a coastal groundwater system. *Water* 9(4):273.

Sae-Ju, J., Chotpantarat, S., and Thitimakorn, T. 2020. Hydrochemical, geophysical and multivariate statistical investigation of the seawater intrusion in the coastal aquifer at Phetchaburi Province, Thailand. *Journal of Asian Earth Sciences* 191:104165.

Sahinci, A. 1991. *Geochemistry of Natural Waters*. Izmir, Turkey: Reform Printing Office, 548.

Sargaonkar, A., and Deshpande, V. 2003. Development of an overall index of pollution for surface water based on a general classification scheme in Indian context. *Environmental Monitoring and Assessment* 89(1):43–67.

Seanego, K. G., and Moyo, N. A. G. 2013. The effect of sewage effluent on the physico-chemical and biological characteristics of the Sand River, Limpopo, South Africa. *Physics and Chemistry of the Earth, Parts A/B/C* 66: 75–82.

Seckin, G., Yilmaz, T., Sari, B., and Ersu, C. B. 2010. Groundwater hydrochemistry at the Mediterranean coastal plains—The case of Silifke, Turkey. *Desalination* 253(1):164–169.

Selle, B., Schwientek, M., and Lischeid, G. 2013. Understanding processes governing water quality in catchments using principal component scores. *Journal of Hydrology* 486:31–38.

Sherif, M., Mohamed, M., Kacimov, A., and Shetty, A. 2011. Assessment of groundwater quality in the northeastern coastal area of UAE as precursor for desalination. *Desalination* 273(2):436–446.

Shi, L., and Jiao, J. J. 2014. Seawater intrusion and coastal aquifer management in China: A review. *Environmental Earth Sciences* 72(8):2811–2819.

Siebert, S., Burke, J., Faures, J.-M., Frenken, K., Hoogeveen, J., Döll, P., et al. 2010. Groundwater use for irrigation—A global inventory. *Hydrology and Earth System Sciences* 14(10):1863–1880.

Simeonov, V., Stratis, J. A., Samara, C., Zachariadis, G., Voutsa, D., Anthemidis, A., et al. 2003. Assessment of the surface water quality in Northern Greece. *Water Research* 37(17):4119–4124.

Souid, F., Agoubi, B., Telahigue, F., Chahlaoui, A., and Kharroubi, A. 2018. Groundwater salinization and seawater intrusion tracing based on Lithium concentration in the shallow aquifer of Jerba Island, southeastern Tunisia. *Journal of African Earth Sciences* 138:233–246.

Stigter, T. Y., Ribeiro, L., and Dill, A. C. 2008. Building factorial regression models to explain and predict nitrate concentrations in groundwater under agricultural land. *Journal of Hydrology* 357(1):42–56.

Sung, K.-Y., Yun, S.-T., Park, M.-E., Koh, Y.-K., Choi, B.-Y., Hutcheon, I., et al. 2012. Reaction path modeling of hydrogeochemical evolution of groundwater in granitic

bedrocks, South Korea. *Journal of Geochemical Exploration* 118:90–97.

Talukder, M. R. R., Rutherford, S., Phung, D., Islam, M. Z., and Chu, C. 2016. The effect of drinking water salinity on blood pressure in young adults of coastal Bangladesh. *Environmental Pollution* 214:248–254.

Telahigue, F., Agoubi, B., Souid, F., and Kharroubi, A. 2018. Assessment of seawater intrusion in an arid coastal aquifer, south-eastern Tunisia, using multivariate statistical analysis and chloride mass balance. *Physics and Chemistry of the Earth, Parts A/B/C* 106:37–46.

Tully, K., Gedan, K., Epanchin-Niell, R., Strong, A., Bernhardt, E. S., BenDor, T., et al. 2019. The invisible flood: The chemistry, ecology, and social implications of coastal saltwater intrusion. *BioScience* 69(5):368–378.

Water Environment Federation and American Public Health Association. 2005. *Standard methods for the examination of water and wastewater*. Washington, DC: American Public Health Association (APHA).

Werner, A. D., Alcoe, D. W., Ordens, C. M., Hutson, J. L., Ward, J. D., and Simmons, C. T. 2011. Current practice and future challenges in coastal aquifer management: Flux-based and trigger-level approaches with application to an Australian case study. *Water Resources Management* 25(7):1831–1853.

Wilcox, LVj. 1955. *Classification and Use of Irrigation Waters*. Washington, DC: USDA.

Yilmaz, T., Seckin, G., and Sari, B. 2010. Trace element levels in the groundwater of Mediterranean Coastal Plains—The case of Silifke, Turkey. *CLEAN - Soil, Air, Water* 38(3):221–224.

Yusuf, K. A., Surukite, O., Abdusalam, I. O., and Majolagbe, A. O. 2013. Assessment of spatial variation of surface water quality in Lagos, using multivariate statistical techniques. *Journal of Environment 2*(4), 94-102.

Zhang, E., Savenije, H. H., Wu, H., Kong, Y., and Zhu, J. 2011. Analytical solution for salt intrusion in the Yangtze Estuary, China. *Estuarine, Coastal and Shelf Science* 91(4):492–501.

Zhao, M., Zeng, C., Liu, Z., and Wang, S. 2010. Effect of different land use/land cover on karst hydrogeochemistry: A paired catchment study of Chenqi and Dengzhanhe, Puding, Guizhou, SW China. *Journal of Hydrology* 388(1):121–130.

Zhu, B., and Yu, H. 1995. The use of geochemical indicator elements in the exploration for hot water sources within geothermal fields. *Journal of Geochemical Exploration* 55(1):125–136.